RF CHARACTERIZATION OF LATEX-COATED PYRAMIDAL ABSORBER

Jeff Guerrieri, Josh Gordon, David Novotny, Jason Coder, Brian Stillwell
National Institute of Standards and Technology
325 Broadway
Boulder, CO 80305

ABSTRACT

We present a test procedure and results that compare RF performance of traditional pyramidal absorber to that with latex coating. Measurements were performed from 5 to 15 GHz, but the same measurement methodology can be applied to other frequency bands. Absorber with protective coating is being used in place of traditional absorber for outdoor antenna measurement facilities to reduce degradation of the absorber performance in harsh environments. Knowledge of the RF performance characteristics of coated absorber is especially necessary when it is used to replace uncoated absorber in an operational antenna measurement facility. Measurements are performed with a simple measurement setup based on a vector network analyzer and broadband horn antennas. Results from bi-static and mono-static measurements are presented.

Keywords: bi-static, latex-coated absorber, mono-static, pyramidal absorber

1. Introduction

This paper describes the measurement techniques and setup for RF characterization of latex-coated pyramidal absorber.[1] The RF performance of the latex-coated absorber is compared to that of the same, non-coated absorber. Measurements were performed with bi-static and mono-static setups using dual ridge horns from 5 to 15 GHz.

2. Measurement Set Up

A reference signal, S_{21ref}, was established for the measurements by use of two dual ridge horns separated by 2 m, illustrated in Figure 1(a). This reference signal level is needed to align the horns in the bi-static and mono-static measurement setups. An accurate boresight alignment of the horns was performed with the overlay imaging aligner technique describe at AMTA 2011[2], shown in Figure 2 .

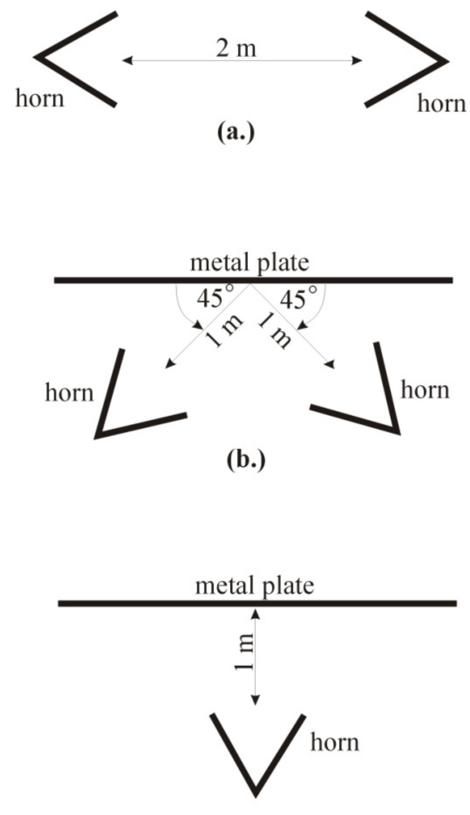

Figure 1. Setup for reference signal (a), setup for bi-static measurements (b), and setup for mono-static measurements (c).

A non-reflective measurement test fixture was constructed from non-metallic foam, shown in Figure 3. For the bi-static measurements the horns were placed at 45 degree angles 1 m from the fixture, illustrated in Figure 1(b). An alignment fixture with guides, shown on the test fixture in Figure 3 was used to the align horns. For the mono-static measurements, a single horn was placed at normal incidence at 1 m from the fixture, illustrated in Figure 1(c). The alignment fixture was used to the aligned the horn.

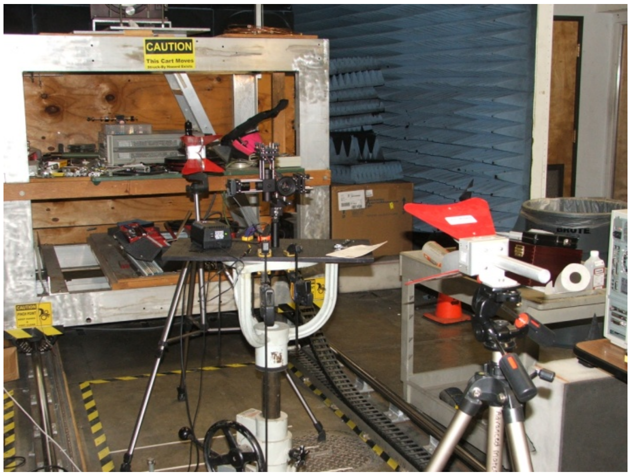

Figure 2. Optical setup for overlay image aligner.

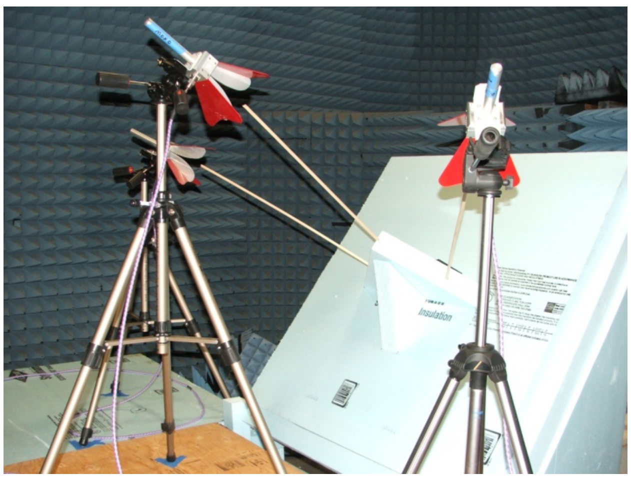

Figure 3. Test fixture with alignment guides for both bi-static and mono-static measurements.

A 1.2 m x 1.2 m (4 ft x 4 ft) metal plate placed in the test fixture, shown in Figure 4, was used as a scattering reference to verify the alignment of the setups for both bi-static and mono-static measurements. The correct distances for the bi-static and mono-static setups can be determined by comparing the time-domain transform of the transmitted signal with that of the direct horn-to-horn signal.

A simple application of the Friis transmission formula and time gating can correct for small differences in distances between setups and assure signal alignment. Starting with the Friis equation:

$$\frac{P_{recv}}{P_{trans}} = |S_{21}|^2 \propto \frac{G_{trans}G_{recv}}{d^2} L_{excess} \quad (1)$$

where S_{21} is the transmission coefficient; G_x are the gains for the transmit and receive antennas; d is the separation distance; and L_{excess} is the loss due to the absorber (L_{excess} = 1 for the maximum transmission cases).

Rewriting (1), we can see that if the distance-transmission coefficient product is a constant, so offsets from the reference distance can be corrected by altering the power level by the distance offset:

$$|S_{21}|^2 d^2 \propto G_{trans}G_{recv}L_{excess},$$

$$\frac{|S_{21test}|^2 d_{test}^2}{L_{test}} = \frac{|S_{21ref}|^2 d_{ref}^2}{1} \propto G_{trans}G_{recv},$$

$$L_{test} = \frac{|S_{21test}|^2 d_{test}^2}{|S_{21ref}|^2 d_{ref}^2}.$$

The data are time gated to remove any secondary reflections leaving:

$$L_{test_{Bi-static}} = \frac{\text{TimeGated}\left[|S_{21test}|^2 d_{test}^2\right]}{\text{TimeGated}\left[|S_{21ref}|^2 d_{ref}^2\right]} \quad (2)$$

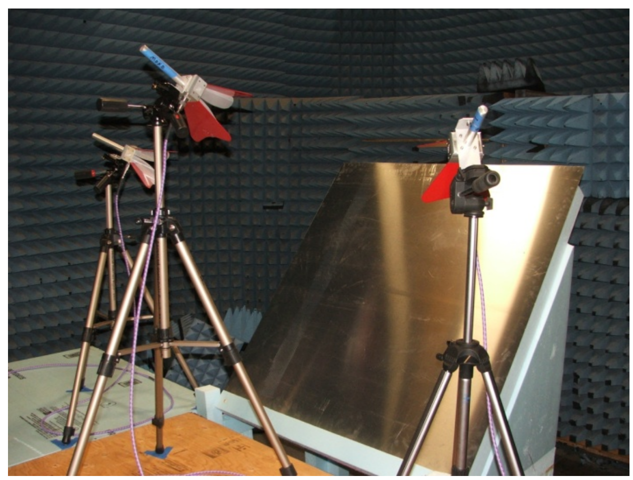

Figure 4 Reference metal plate showing both bi-static and mono-static setups.

Figure 5(a) shows that the time-domain transform of the bi-static signal, $S_{21\ bi\text{-}static\ metal}$, is earlier in time than the horn-to-horn signal, $S_{21\ ref}$, by 0.017 ns. This equates to a distance of 5.05 mm, therefore, the bi-static test distance should be 1.995 m. This is corrected with a 0.017 ns time delay, shown in Figure 5(b). The match in magnitude for the two signals also indicates polarization alignment.

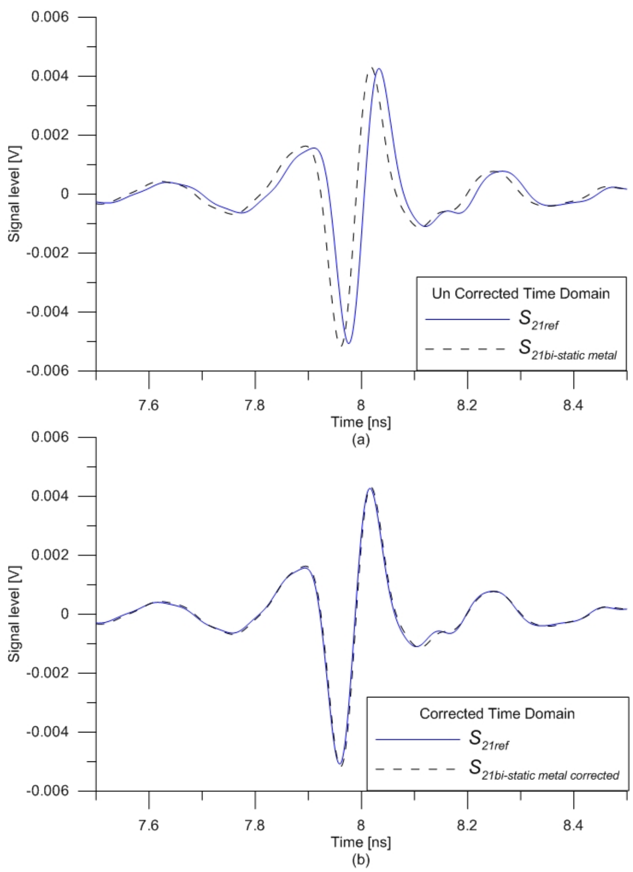

Figure 5. Uncorrected bi-static time-domain signal (a) and corrected bi-static time domain signal (b).

The mono-static measurement is also compared to S_{21ref} to insure the alignment is correct and that propagation is normal to the plate. A slightly different method is required for the mono-static case. The S_{11} signal contains the reflection from the cable-to-horn interface as well as the reflections from the plate. A background subtraction, where there is no target or support structure in front of the antenna is used to subtract out the systematic reflections from the antenna:

$$L_{mono-static} = \frac{\mathrm{TimeGate}\left[\left|S_{11test} - S_{11background}\right|^2 d_{test}^2\right]}{\mathrm{TimeGate}\left[\left|S_{21ref}\right|^2 d_{ref}^2\right]} \;. \quad (3)$$

Figure 6(a) shows is the time-domain transform of the mono-static measurement showing all the systematic reflections from the antenna. These are removed by subtracting a measurement into empty space (without the plate or test stand). Figure 6(b) shows the area of interest from (a), similar to the bi-static case. The subtracted reflections show a 0.065 ns delay with respect to the reference. This equates to a 19.5 mm increase in the propagation path with respect to S_{21ref}. A distance correction, d_{test}, of 2.015 m, is used to correct the mono-static measurements, shown in Figure 6(c).

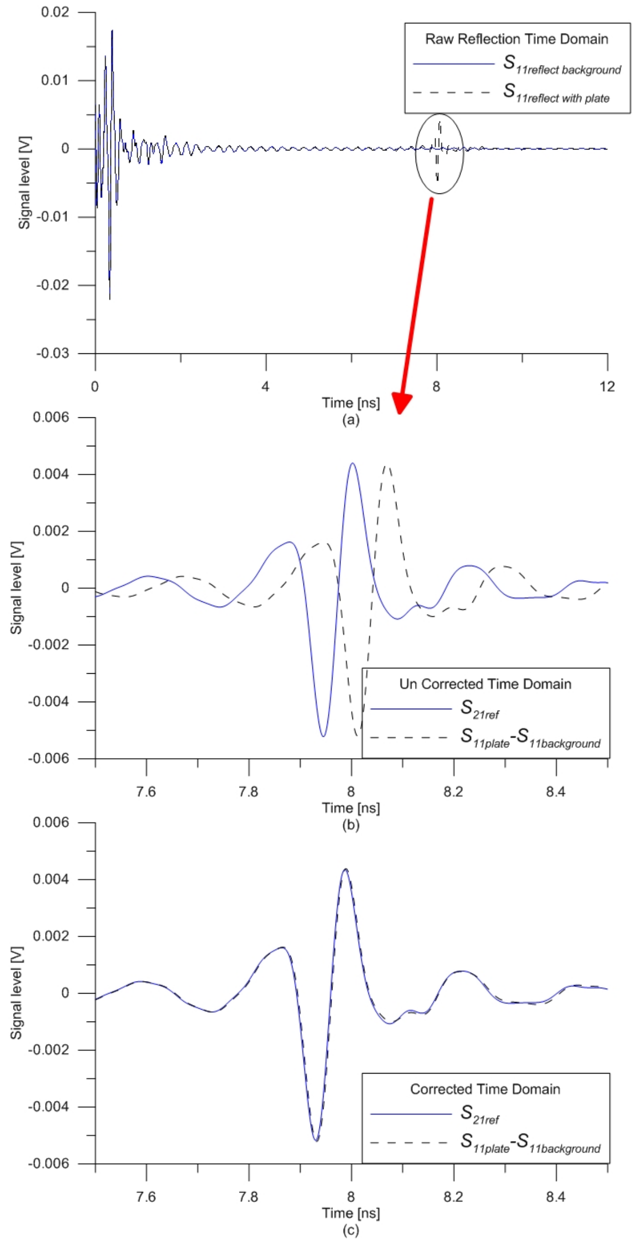

Figure 6. Raw mono-static time-domain signal (a), uncorrected mono-static time domain signal (b) and corrected mono-static time domain signal (c).

3. Measurements

Bi-static and mono-static measurements were performed without the test fixture to establish the measurement background noise floor. Then the measurements were also performed on just the test fixture.

A 1.2 m x 1.2 m (4 ft x 4 ft) test sample of non-coated 8 inch absorber was constructed and placed in the sample fixture, shown in Figure 7. The bi-static and mono-static measurements were performed.

A 1.2 m x 1.2 m (4 ft x 4 ft) test sample of the latex coated 8 inch absorber was constructed and placed in the test fixture, shown in Figure 8. The bi-static and mono-static measurements were performed on the coated absorber.

Figure 7. Non-coated absorber in the test fixture.

Figure 8. Latex-coated absorber in the test fixture.

4. Measurement Results

The graph in Figure 9 displays the frequency-domain results for the bi-static measurements. The measurement results were normalized to that of the metal plate. These measurements have an uncertainty of ±1 dB. The measurements results with just the test fixture are only -30 dB.

With the non-coated absorber sample on the test fixture the measured results are -34 dB from 5 to 8 GHz and better than -39 dB from 8 to 15 GHz. The measured results for the coated absorber in the fixture are similar to that of the traditional absorber. From 5 to 9 GHz the measured results are -33 dB. From 9 to 15 GHz the reflection levels are lower than -40 dB.

The graph in Figure 10 displays the frequency-domain measurement results from the mono-static measurements. These measurements results were also normalized to that of the metal plate. The measurement results for the test fixture are -35 dB.

The measurement results for the non-coated absorber in the test fixture are lower than -40 dB from 5 to 15 GHz. The results for the coated absorber are lower than -37 dB from 5 to 7 GHz and lower than -40 dB from 7 to 15 GHz.

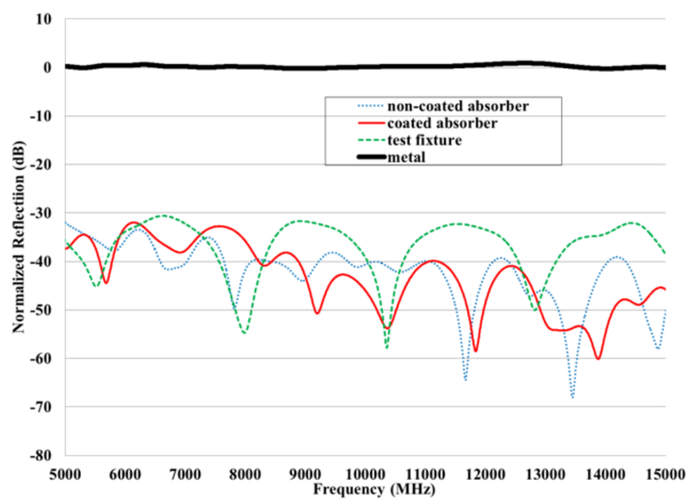

Figure 9. Bi-static measurement results.

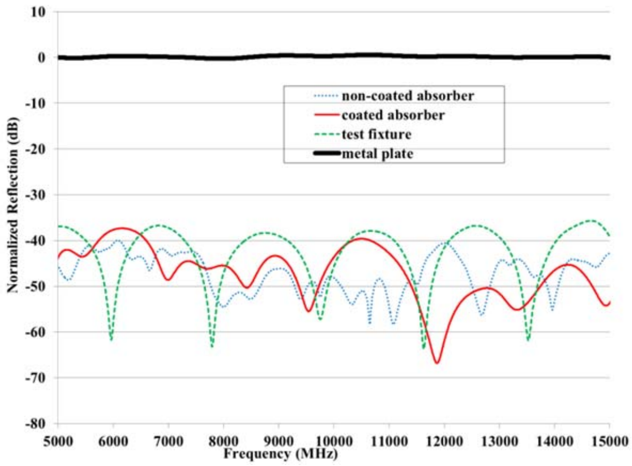

Figure 10. Mono-static measurement results.

5. Uncertainty

The major contributors to the uncertainty are horn alignment, polarization mismatch and edge diffraction due to the limited size of the metal plate. This is seen in the difference between bi-static and mono-static measurements of the metal plate, shown in Figure 11, which show an uncertainty of 1 dB.

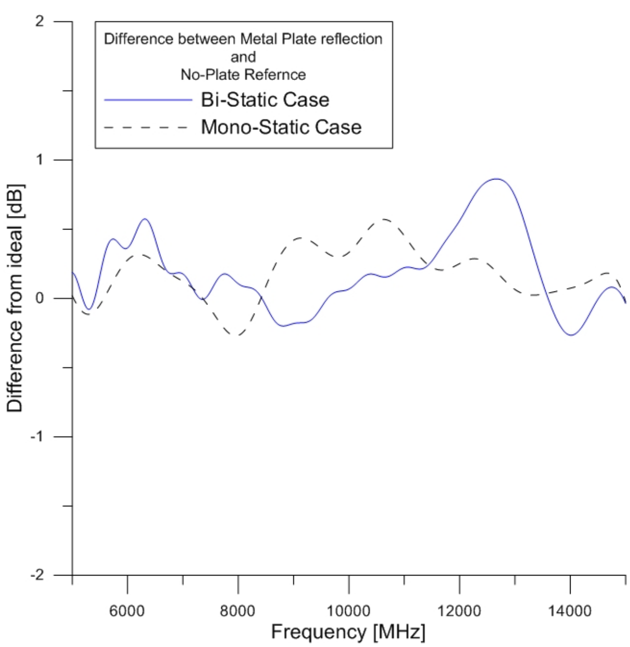

Figure 11. The difference between the metal plate and the reference measurements.

6. Summary

This paper discusses results for RF performance characterization of 8 inch pyramidal absorber with and without latex coating. A proven technique was used to perform measurements from 5 to 15 GHz. The results of these measurements do not indicate degradation of RF performance for the given latex-coated absorber.

7. References

[1] Novotny, D. R., Johnk, R. T., Ondrejka, A., "Low Cost Broadband Absorber Measurements", AMTA Proceedings 2000, pp. 357-362, Philadelphia, PA.

[2] Gordon, J. A., Novotny, D. R., "Alignment of Two mmWave Antennas Using an Improved Optical Alignment Tool", AMTA Proceedings 2011, pp. 245-250, Englewood, CO.

8. Acknowledgements

The authors wish to thank the U. S. Department of the Army's Electronic Proving Grounds in Ft. Huachuca, Arizona for sponsorship of this research project.